

RESULTS FROM THE FIRST INTEGRATED SYSTEM TESTS OF THE GRAVITY PROBE B EXPERIMENT

M. A. TABER, D. BARDAS, S. BUCHMAN, D. B. DEBRA, C. W. F. EVERITT, D. K. GILL,
G. M. GUTT, G. M. KEISER, J. M. LOCKHART*, B. MUHLFELDER, B. W. PARKINSON,
R. A. VAN PATTEN, J. P. TURNEAURE, Y. M. XIAO
W. W. Hansen Experimental Physics Laboratory, Stanford University, Stanford, CA 94305-4085, USA

and

R. T. PARMLEY, D. J. FRANK, G. M. REYNOLDS
*Research & Development Division, Lockheed Missiles & Space Company, Inc., 3251 Hanover Street,
Palo Alto, CA 94304, USA*

ABSTRACT

The Gravity Probe B Relativity Gyroscope Experiment (GP-B) will provide a precise and controlled test of Einstein's General Theory of Relativity by observations of the precession of nearly perfect gyroscopes in Earth orbit. For gyroscopes in a 650 km polar orbit the theory predicts two orthogonal effects, known as the geodetic and frame-dragging precessions, with calculated rates of 6.6 arc-s/yr and 0.042 arc-s/yr respectively. The goal of the experiment is to measure the geodetic effect to better than 0.01% and the frame-dragging effect to better than 1%. This paper describes the First Integrated System Tests (FIST) which is the first attempt of the GP-B Program to design, build, integrate, and test hardware that is in many respects prototypical of the flight instrument. Results from the successful completion of the first two segments of FIST, which include the operation of two gyroscopes and a number of engineering tests, are summarized.

1. Introduction

1.1 *The Relativity Gyro Experiment*

1.1.1 The Experimental Concept

The Gravity Probe-B Relativity Gyroscope Experiment (GP-B) will provide a precise and controlled test of Einstein's General Theory of Relativity by observations of the precession of nearly perfect gyroscopes with respect to a distant guide star (Rigel) while in Earth orbit (Fig. 1). For gyroscopes in a circular polar orbit with the gyro spin vectors in the direction of the guide star and the guide star in the orbital plane, the theory predicts two orthogonal effects, the geodetic and frame-dragging precessions.¹ For a 650 km orbit, the former has a calculated rate of 6.6 arc-s/yr and occurs in the plane of the orbit, and the latter has a predicted rate of 0.042 arc-s/yr and causes the gyros to precess out of the plane

of the orbit. The goal of the experiment is to measure the geodetic effect to better than 0.01% and the frame-dragging effect to better than 1%.²

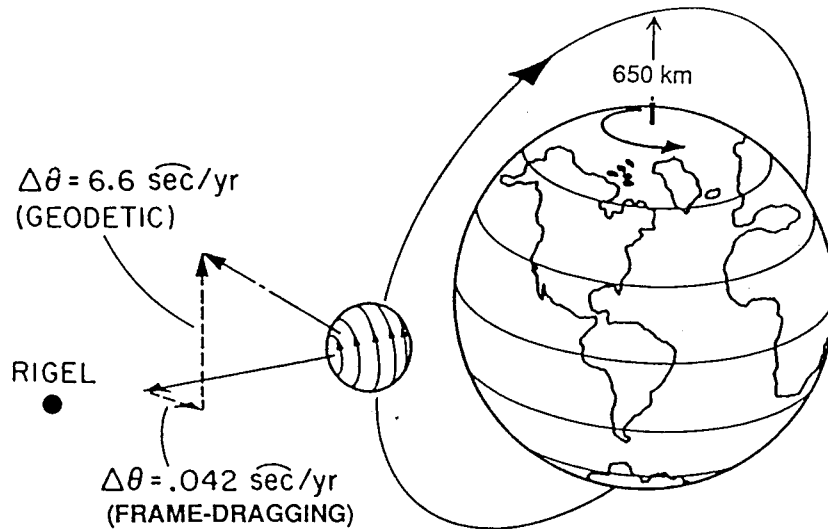


Figure 1. Concept of the experiment showing the precession of an orbiting gyroscope with respect to the line of sight to the guide star. In practice, corrections must be made for the star's proper motion and the difference between its apparent and actual position.

1.1.2 Key GP-B Technologies

The extremely small values of the precession rates to be measured places strict requirements on the alignment and the pointing stability of the gyro readouts with respect to Rigel, on the level of disturbance torques on the gyroscopes, and on the noise characteristics of the readouts. These requirements in turn put severe constraints on the experimental design and on the choice of technologies. The following is a summary of the key technologies which have been selected and the requirements which are necessary for the GP-B experiment:³

*Electrostatically suspended gyros using gas spinup and high precision fused quartz rotor and housing*⁴ (Fig. 2). The rotors, which are approximately 3.8 cm in diameter and made out of fused quartz with a niobium coating, require a density variation of $< 10^{-5}$, a peak-to-valley asphericity and mass unbalance of $< 50 \text{ nm}$, and an upper limit on the electric charge of 50 pC during operation. Spinup to approximately 170 Hz is accomplished by flowing He gas through a spin-up channel located in one of the housing halves. Gas which escapes the spin-up channel is pumped away through an auxiliary channel and vent holes.

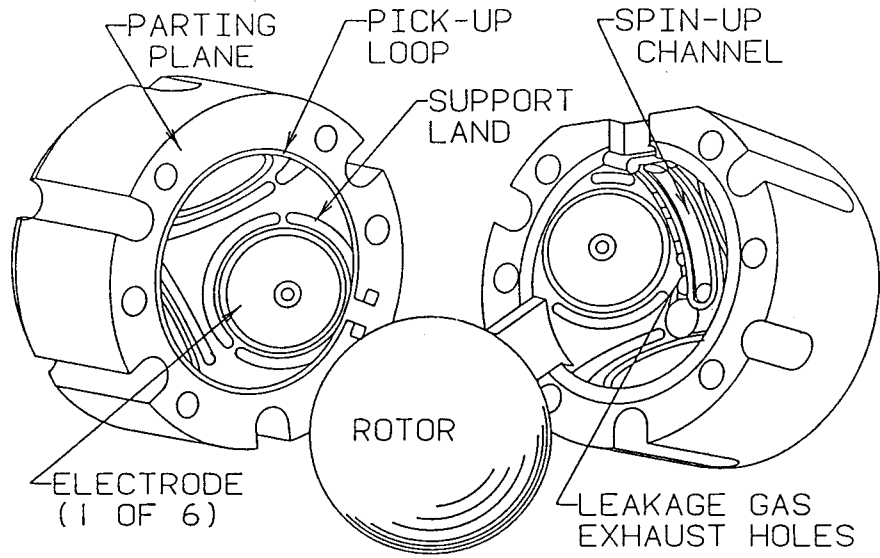


Figure 2. Exploded view of gyroscope rotor and housing. The rotor is coated with 2.5 μm of Nb.

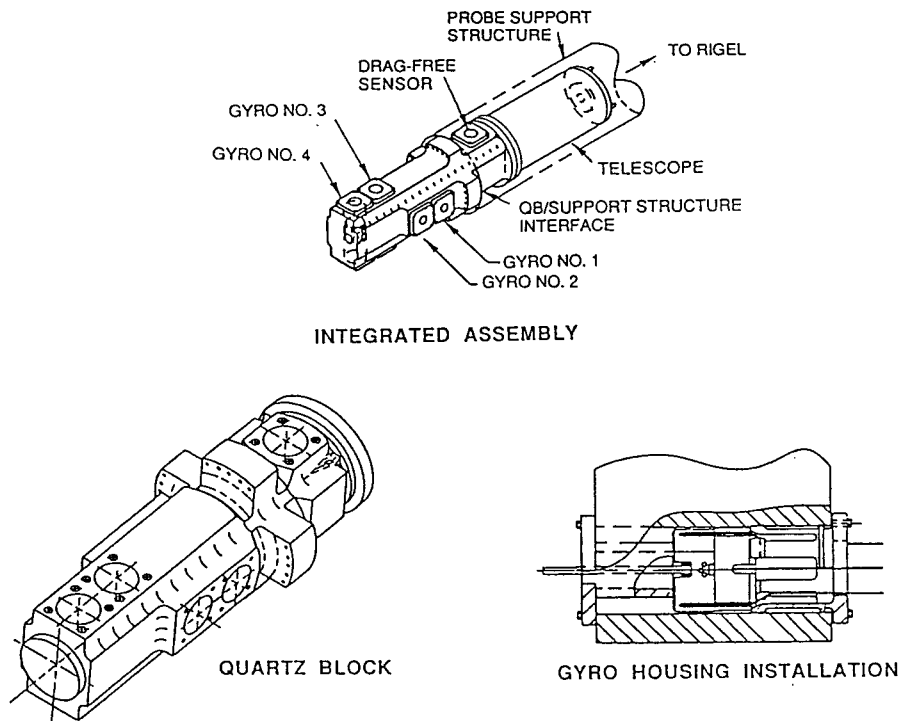


Figure 3. The Quartz Block Assembly (QBA), consisting of the Quartz Block, four gyros and a proof mass, together with the telescope.

*London moment readout using dc SQUIDs.*⁵ The direction of the spin axis of the gyro can be determined by means of the co-aligned London magnetic dipole moment⁶ produced by the thin superconducting coating on the surface of the rotor. This moment is measured by a dc SQUID (Superconducting QUantum Interference Device) which is coupled to the gyro by a superconducting coupling circuit. The pickup loop, which is a thin-film structure deposited on the parting plane of the housing, is oriented with its normal orthogonal to the line of sight to Rigel. With the satellite rolling around the line of sight (10 minute roll period), precession of the gyro will cause a London-moment signal to appear at the SQUID output at the roll frequency. The phase of this signal will indicate the direction of precession.

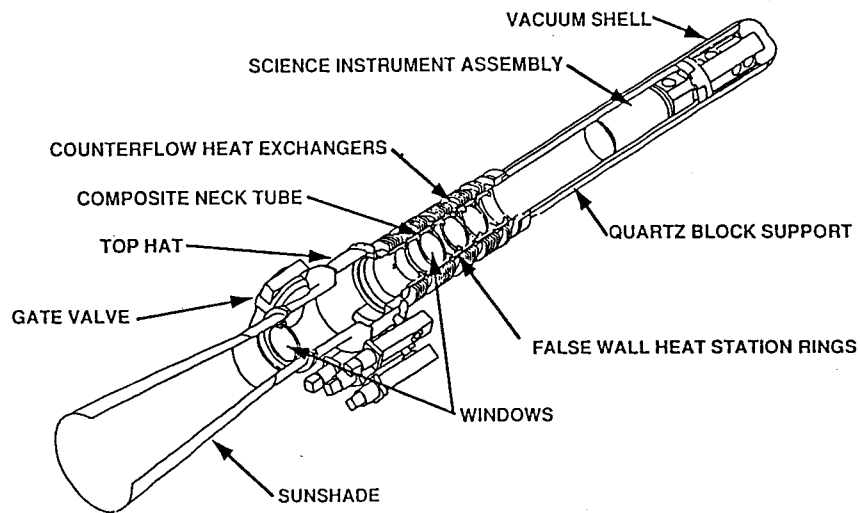


Figure 4. The cryogenic probe, which includes the Science Instrument Assembly.

Superfluid He thermal environment and optically-contacted fused quartz construction. All critical components of the experiment including the telescope⁷ are constructed of fused quartz and are integrated by means of optical contacting into the Quartz Block Assembly (QBA) (Fig. 3). The low thermal coefficient of expansion of fused quartz together with the thermal stability and uniformity afforded by operation at superfluid He temperature (1.8 K) assure the mechanical stability needed for the experiment. The Science Instrument Assembly (SIA, which includes the QBA, telescope, and SQUID assemblies) is mounted on a cryogenic probe and enclosed by a vacuum shell (Fig. 4). The probe provides vacuum and thermal isolation, optical access to the telescope, and mechanical, thermal and electrical support for the SIA. The probe is inserted into the central well of the dewar (Fig. 5) which maintains the 1.8 K thermal environment by means of an annular tank of superfluid He. The tank is vented to space by means of a porous plug.⁸

Zero-g satellite rolled around line of sight. By sensing the relative position of a proof mass located in the QBA near the center of mass of the satellite and adjusting the

venting of boiloff He gas through proportional thrusters, the satellite can be flown in a nearly drag-free condition ($\leq 10^{-11}$ g).⁹ This reduces the suspension forces and their associated torques to acceptably low values. In addition, rolling the satellite around the line of sight averages residual transverse torques which originate in the satellite, and encodes the precession signal at the roll frequency, reducing the effect of $1/f$ noise in the readout. The absolute roll phase will be determined by an external star blipper that is stably linked to the orientation of the QBA.

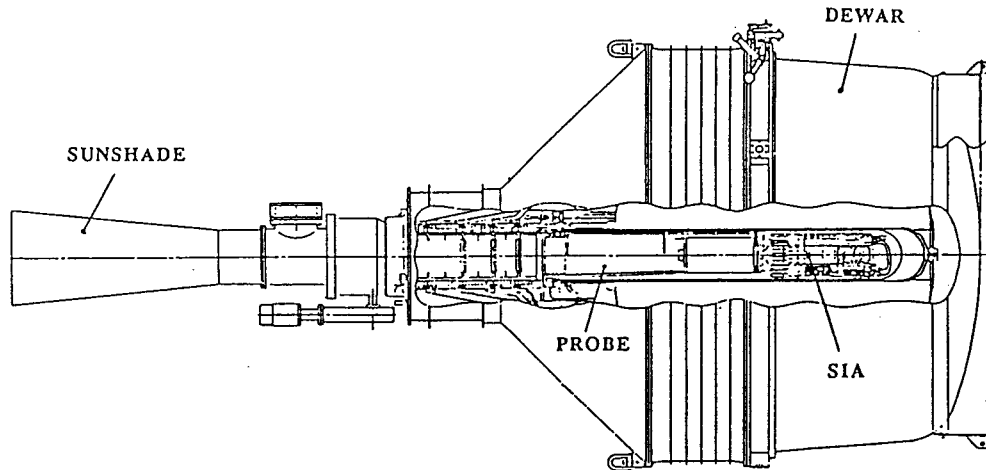


Figure 5. The integrated payload consisting of the probe in the science mission dewar.

Ultrahigh vacuum. The cryogenic probe should be capable of maintaining the gyros in an ultrahigh vacuum ($< 10^{-11}$ torr) after the spin-up process and a subsequent low-temperature bakeout to ~ 7 K.¹⁰ This pressure is necessary to keep gas drag torque, and more importantly, any differential damping torque due to pressure gradients, to an acceptable level.

Ultralow magnetic field environment. The ambient dc magnetic field in the vicinity of the the gyros should be maintained at $\sim 10^{-7}$ G in order to keep trapped flux in the rotors and magnetic torques to a tolerable level. In addition, external ac magnetic fields (i.e., the Earth's field) must be attenuated by a factor of 10^{13} at the pickup loops to avoid signal contamination. These requirements can be met by means of a high-permeability shield outside the dewar well (optimized for low temperature use), a degaussed superconducting Pb-foil shield¹¹ inside the well, and local superconducting Nb shields around each gyro. Flux trapped in superconducting components located in the probe (including the local shields and the gyro rotor coatings) can be flushed by uniformly heating the SIA above their critical temperatures and slowly recooling to 2 K.

Cold-dewar integration. Installation of the Pb-foil shield is an elaborate and lengthy process that must be accomplished prior to integration of the probe into the dewar.

Once the shield is established, the dewar must be kept continuously cold. This imposes a subsidiary requirement that the probe be cooled down by insertion into the cold dewar with liquid He in the dewar well as the cryogen. This is accomplished by means of a large airlock and piston arrangement (Fig. 6). Once the probe is fully inserted, complete mechanical and thermal integration is accomplished by means of three dogging mechanisms located at the bottom of the neck region of the dewar and spring-loaded thermal links located at heat exchangers situated on the neck of the probe.¹² After the probe is fully integrated into the dewar, the liquid helium remaining in the well can be pumped out and the well evacuated.

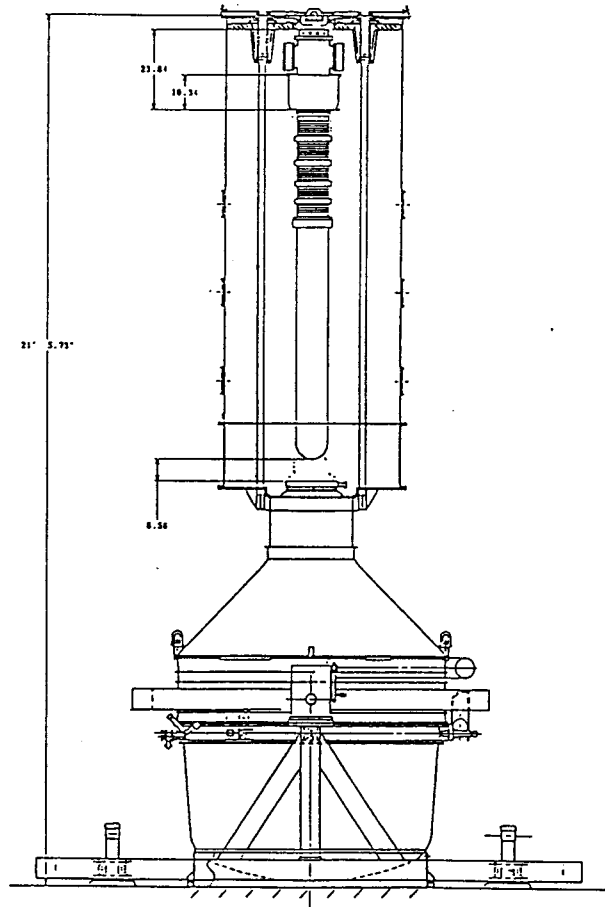


Figure 6. Probe integration with the dewar by means of an airlock and piston assembly.

1.2 GP-B Hardware Development Program

The overall GP-B hardware development program is based on an approach of incremental prototyping involving three generations of hardware (Fig. 7). The design and fabrication of the probe and dewar are the responsibility of Lockheed Research and Development Division, and the SIA development, including that of the telescope, gyros,

and readout, is being done by Stanford University. Functional testing of the integrated systems (dewar and probe with the SIA) is being done at Stanford with Lockheed support.

In addition to the incremental prototyping of Science Mission hardware, Stanford, with Lockheed support, is building a room-temperature Shuttle Test Unit (STU) which will be flown on two space shuttle missions for the purpose of testing GP-B gyros and their suspension systems in a nearly zero acceleration environment. STU will have the capability of levitating, spinning up, damping, and accurately measuring the spin speed of either or both of two gyros.

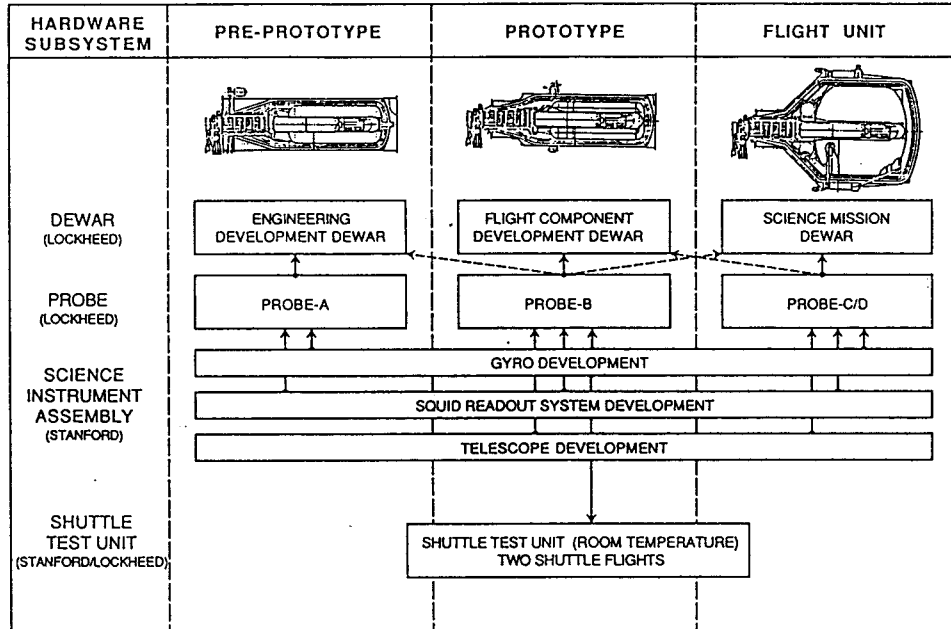


Figure 7. Schematic representation of the GP-B hardware development program. All probes after Probe-A will fit in any of the dewars.

2. First Integrated System Tests: FIST

The First Integrated System Tests represents the culmination of the development of the first generation of prototypical hardware¹³. This hardware consists of the Engineering Development Dewar (EDD), Probe-A, and a prototypical SIA (Fig. 8). Although this system is prototypical in many essential regards, a number of deviations from current flight hardware requirements and design were allowed for reasons of economy and practicality. Probe-A and the EDD design are discussed elsewhere in this volume,¹² and the deviations in the SIA are shown in Table 1.

2.1 FIST Segments and Their Objectives

For organizational purposes, FIST was divided into three segments: FIST-A, -B, and -C. The first two of these segments were completed in the summer of 1990. FIST-A & B are distinguished from FIST-C by the fact that a defect in the EDD (a leak between the well and the guard vacuum) prevented the use of liquid helium in the well and precluded the establishment of an ultralow field shield and the use of the cold-insertion process. Thus for FIST-A & B the probe was first integrated into the dewar and then both were cooled down together.

FIST-A involved the basic system integration and test. Its purpose was to uncover any integration problems and to quickly check the basic functionality of the integrated system. The goal was to verify functionality of all major aspects of the system and to achieve both gyro and SQUID readout operation (using flux trapped in the rotor from the approximately 1 mG ambient field) at 4.2 K He tank temperature. In addition, FIST-A afforded the first opportunity to verify many of our integration and operation procedures (excepting cold insertion and superfluid He operations) as well as verify and test support equipment and facilities.

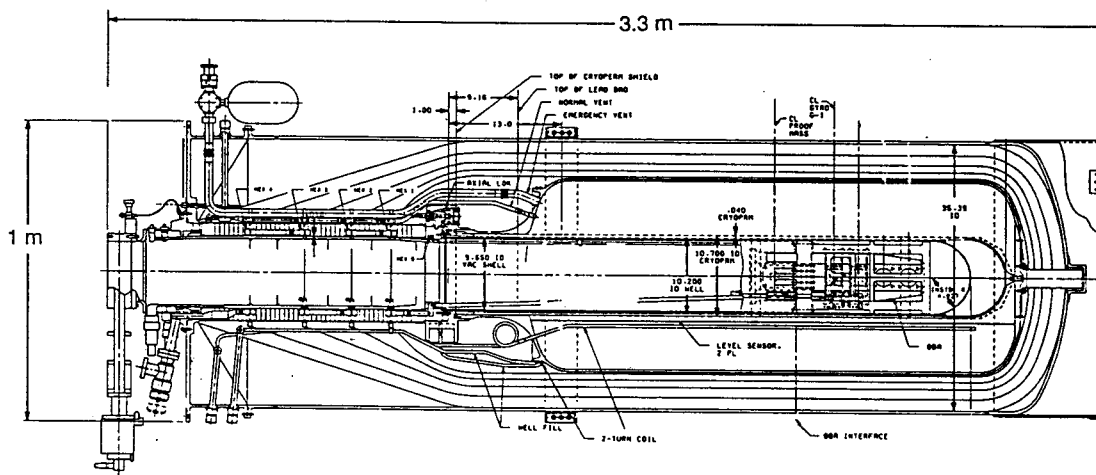


Figure 8. The integrated FIST instrument package. Normal operational orientations are with the dewar axis vertical and tilted 52.6° from the vertical.

Table 1. Deviations of the FIST Science Instrument Assembly from the Science Mission design.

Sub-Assembly	FIST	Science Mission
Gyros	2 with no caging or charge control	4 with caging and UV charge control
SQUIDs	3 rf SQUIDs (one as a magnetometer) with simplified coupling circuits and one test dc SQUID	dc SQUIDs for all gyro readouts
Proof Mass	none	included
Telescope	none	included

FIST-B involved more detailed engineering studies which could be undertaken provided that the results from FIST-A indicated that they were possible and useful. These tests involved thermal, gas flow, and vacuum properties of the probe, ac magnetic shielding factor, operation at superfluid He temperatures, and high speed (50 Hz) spin up of one of the gyros. The overall goal for FIST-B was to provide information to check some of the engineering models used in the design of the probe and the SIA and to point up any significant problems which should be corrected in the probe-B design.

FIST-C will be undertaken once the EDD has been repaired and will focus primarily on cold insertion and low field tests. It will afford the first opportunity to establish an ultralow field superconducting shield in a full-scale prototypical environment. In addition, it will be the first opportunity to fully test the airlock and the cold-insertion procedures. Once the probe is fully integrated into the dewar, a variety of tests will be performed, but the primary emphasis will be on flux-flushing and measuring the trapped flux levels in the gyro rotors.

2.2 Major Results from FIST-A/B

2.2.1 Successful Integration and Cryogenic Operation

One of the most significant accomplishments of FIST was to successfully complete the full integration process without any major difficulties. This success is largely attributable to careful planning and the use of integration rehearsal tests for integration of the QBA into the probe and the integration of the probe into the dewar. Two integration rehearsal probes were fabricated by Lockheed for these purposes. Many of the integration facilities, fixtures, and procedures appear to be sufficient for future generations of hardware with only minor modifications. For example, alignment of the gyros in the quartz block was accomplished with sufficient accuracy to meet science mission requirements. Figures 9-11 show various steps in the integration process and the final configuration of the integrated system including vacuum support equipment.

Cool down and the thermal performance of the integrated probe/dewar system were consistent with expectations. Cool down and fill of the tank (400 liters capacity) took less than 1500 liters of liquid helium starting from room temperature, and the system came into thermal steady state in approximately 26 hours. The steady-state temperature profile and critical interface thermal resistances were generally consistent with the thermal model at both 4.2 K and 1.8 K bath temperatures. With the bath at 4.2 K and no power dissipation in the probe, the temperature at the QBA ran between 4.5 and 5 K depending on the helium level, and with the bath at 1.8 K, the temperature was 2.2 K.

2.2.2 Vacuum and Gas Conduction Performance

The gas conductance properties of the probe are important for the gyro spin-up process. The bulk of the spin-up gas (on the order of 90%) is exhausted in viscous flow through lines which pass up the probe, and through counterflow heat exchangers in the neck region which help cool the incoming gas. The pressure drop associated with the exhaust lines should not be too large because it adversely affects the asymptotic spin speed and the gas leakage rate. Tests in FIST found that the exhaust line pressure was significantly larger than required (0.8 torr instead of 0.3 torr for 2 mg/s flow). The reason for this is that the exhaust lines had been designed for a higher pressure regime with a maximum flow rate of 60 mg/s instead of the new baseline flow rate of 2 mg/s. The exhaust lines for Probe-B have been designed to achieve the required pressure drop at the lower flow rate.

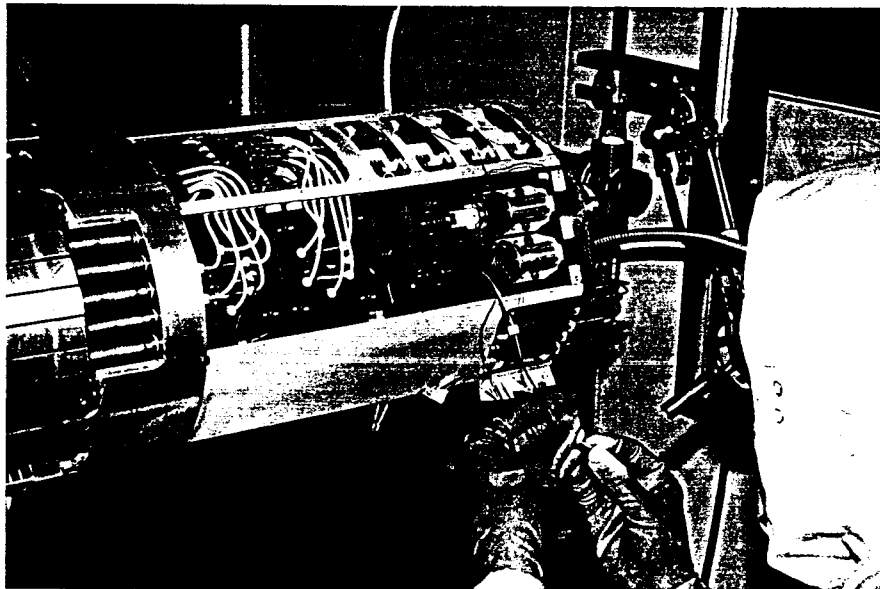


Figure 9. Integration of the FIST Science Instrument Assembly in a class 10 environment.

In addition to the exhaust lines, the molecular flow conductance of the probe itself is important because the gas that leaks out of the spin-up channel must be pumped away fast enough to avoid its electrical breakdown by the high-voltage suspension system. In space, this gas is simply vented through a gatevalve on the top of the probe. During ground test, the probe is pumped on by a turbomolecular pump system which has a pumping speed of ~ 3100 liters/sec for He. FIST test results indicated that the probe gas conductance was sufficient to meet our ground-test requirement (which is more difficult than in space because of the higher suspension voltages) even with the total pumping speed being less than it will be in space because of the finite speed of the pump system.

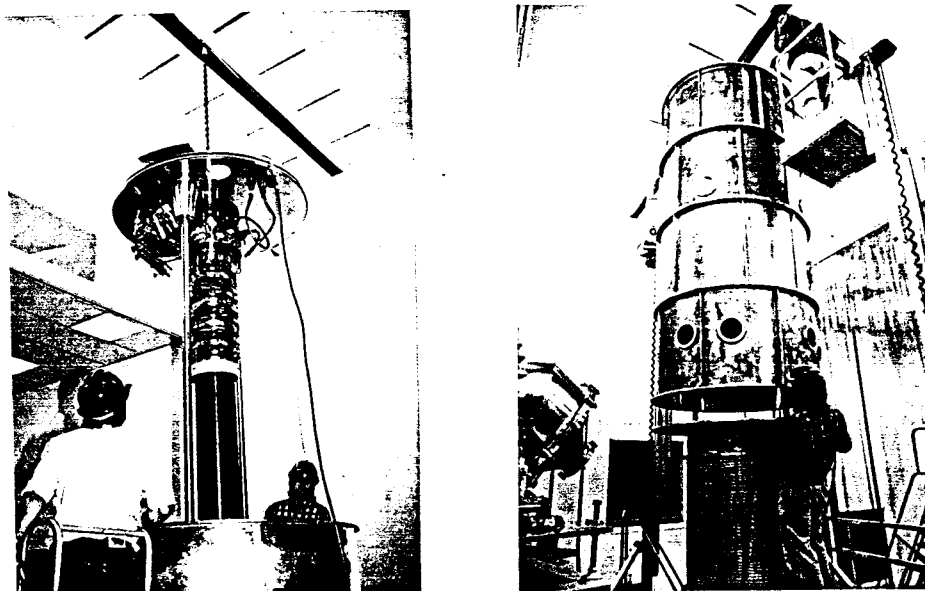


Figure 10. Left: Integration of the probe and piston assembly into the airlock. Right: Lowering the airlock with probe inside onto the dewar.

As noted earlier, there is also a requirement that the pressure in the vicinity of the gyros be $< 10^{-11}$ torr after spin up and a low-temperature bakeout to approximately 7 K. The effectiveness of this technique had been demonstrated earlier on another apparatus.¹⁰ When we attempted this procedure during FIST-B, we were not able to reach a pressure lower than 4×10^{-9} torr. The probable reason for our failure to reach lower pressure was that only the QBA and the lower portion of the quartz block support structure could be heated by the bakeout process. This represents a small fraction of the total probe area; to be effective in a bakeout, the fraction of bakeable area should be close to unity. The design of Probe-B will substantially increase the fraction of bakeable area by adding heaters to the vacuum shell and an annular sintered cryopump located just below the neck region.

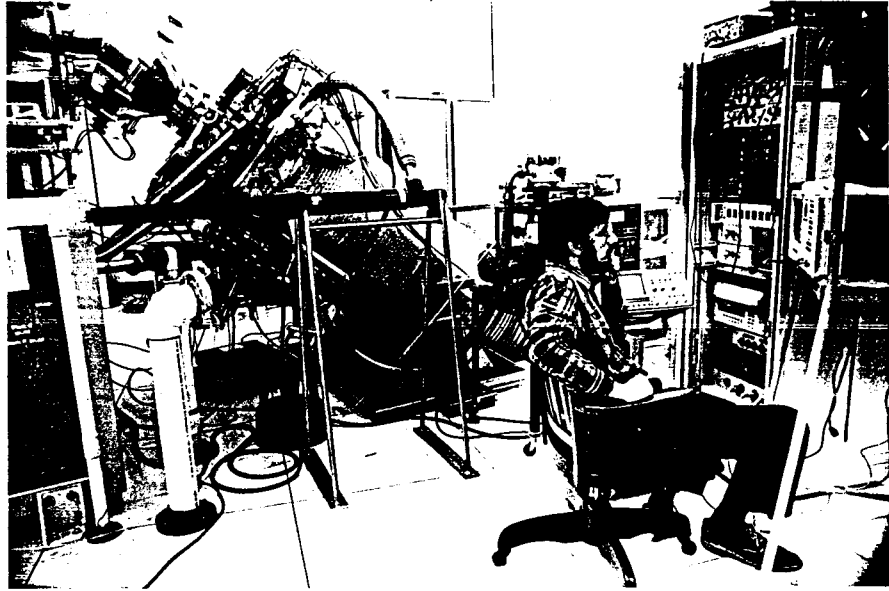


Figure 11. Probc-A and EDD in their integrated test configuration. The tilted orientation places the gyro spin axes parallel to the Earth's axis of rotation which simplifies gyro performance analysis. The large unit on the left contains the leakage gas pump system for pumping on the probe as well as the manifolding and control valving for the spinup gas supply and exhaust systems.

2.2.3 Gyro Operation

FIST represents the first time that two gyros have been tested together to determine whether there are any problems associated with the simultaneous operation of multiple gyros. During FIST-A/B both gyros were spun to 3-5 Hz on numerous occasions (13 times total) with simultaneous operation occurring several times. We accumulated more than 500 hours of trouble-free operation on both gyros, and, in general, found the gyros performed at least as well, if not better, than they did in acceptance tests. No interaction could be detected between gyros except for the increased gas damping of the first gyro when the second gyro was being spun up. Figure 12 shows spin speed vs. time data taken from one test; the dramatic increase in the damping rate caused by the addition of gas on two occasions can clearly be seen.

In addition to the routine low-speed tests, one gyro was spun to 50 Hz with 7 K gas during 1.8 K operation to provide data for our spin-up model. The data from this test are shown in Fig. 13. The asymptotic spin speed estimated from these data is 57 Hz with a characteristic time of 19 min. The reasons for the relatively low asymptotic speed are the low flow rate (1.5 instead of 2 mg/s) and the high pressure drop in the exhaust line noted above.

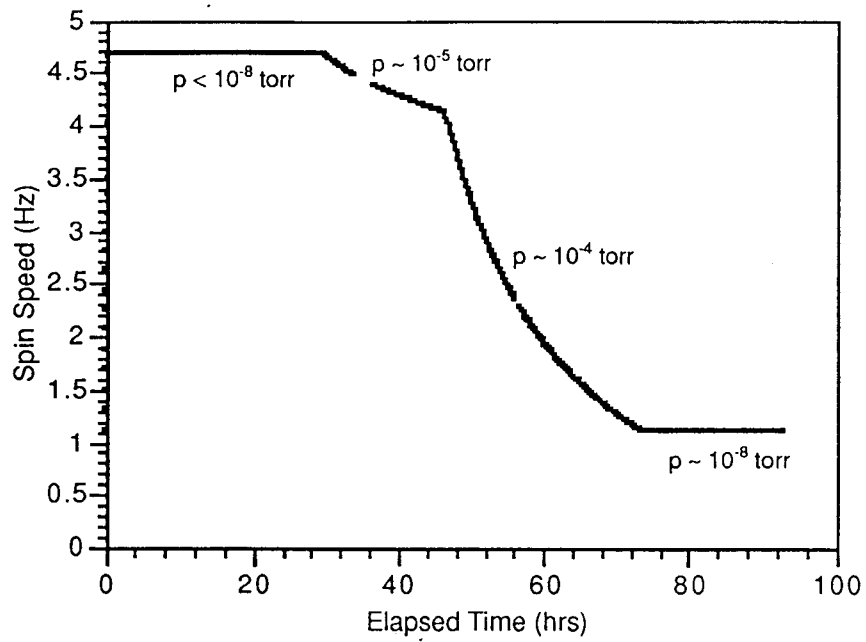


Figure 12. Spin speed data from gyro #1. The four different regions correspond to different pressures of He gas in the probe.

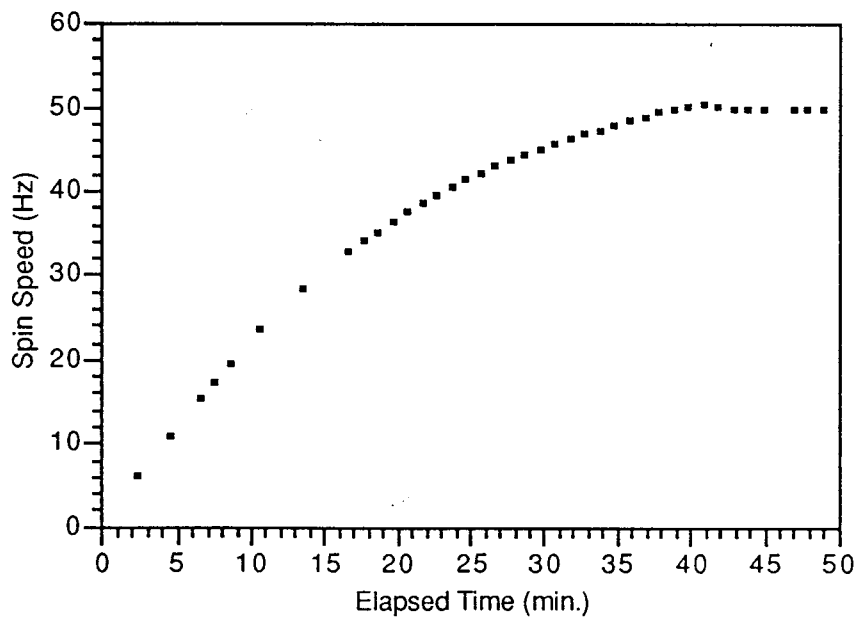


Figure 13. Spin up of gyro #1 to 50 Hz. Gas flow rate was 1.5 mg/s at a temperature of 7 K.

2.2.4 SQUID Readout Operation and ac Shielding Factor

The readout loops of both gyros in FIST were connected to rf-biased SQUIDs¹⁴ via coupling circuits which were optimized for ~ 1 mG trapped-flux readout under ground test conditions. The SQUID sensor for gyro #1 failed on cool down, but the readout for gyro #2 functioned well. All of the functional SQUIDs, including SQUID #3 (utilized as a magnetometer by being coupled to the readout loop on a rotorless gyro housing in the third gyro position) and the shorted dc SQUID, demonstrated very low incidence of flux jumping even during gyro operation. One practical difficulty encountered in gyro readout, however, was that power dissipation in the gyro would heat the housing sufficiently to drive the bond between the thin-film pickup loop and the coupling wires normal when the bath temperature was at 4.2 K. This was not a serious problem because the resistance of the bond was low enough that even low-frequency pendulation of the rotor was observable through ac coupling. In addition, the readout circuits are completely persistent when the bath is operated at 1.8 K. In space, the dissipation issue becomes completely negligible.

As an example of the readout data obtained, Figure 14 shows the trapped flux signal from gyro #2 both after initial cool down and after flux flushing. The initial trapped flux was highly nonuniform as evidenced by the high harmonic content in the SQUID signal; after heating and slowly recooling the gyro, the trapped flux became much more uniform and the signal more sinusoidal.

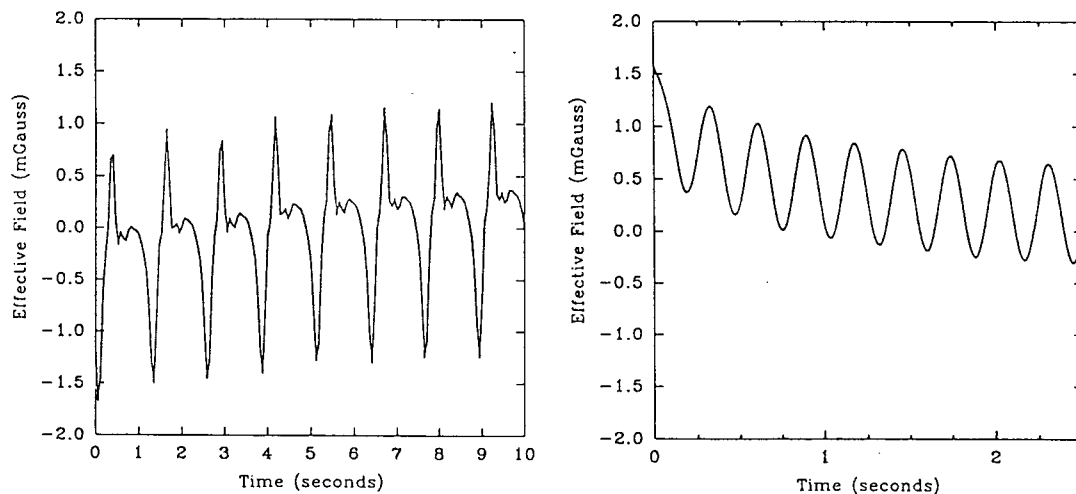


Figure 14. Trapped flux data from gyro #2 taken before (left) and after flux flushing (right). The effective field shown on the ordinate corresponds to the equivalent uniform field which would produce the plotted signal. These signals have been processed to compensate for ac signal coupling.

The presence of a magnetometer pickup loop in the gyro #3 position allowed us to attempt to measure the ac magnetic field attenuation factor. A pair of 6 ft. diameter field coils was set up to apply an external 0.02 Hz ac magnetic field which was monitored with a fluxgate magnetometer. The spectral analysis of the resulting data from SQUID #3 is shown in Figure 15. Since no signal is observable at the applied field frequency, the SQUID noise level is used to set a lower limit on the attenuation factor of 2×10^{11} . This is to be compared with an expectation of $\sim 10^{13}$ as the attenuation factor for the circumstances under which this test was made. We are planning to improve on this measurement in FIST-C by increasing the coupling between the pickup loop and the SQUID.

3. Conclusions

The results of FIST-A/B have revealed a high degree of functionality for a first integrated system test and confirm many aspects of the system design. Problems which have been found so far do not appear to be significant. Low-field aspects of the system will be tested in FIST-C which should be underway in 1992.

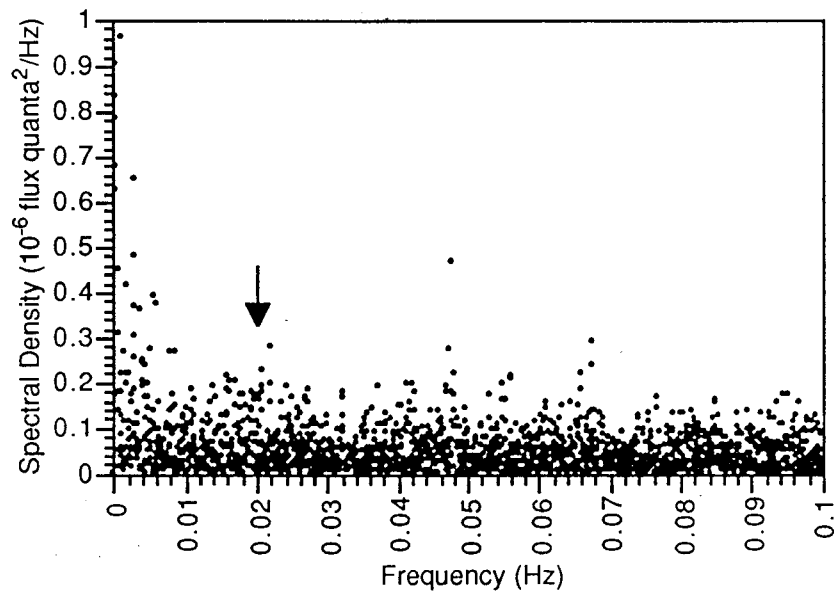


Figure 15. Power spectral density of magnetometer data obtained during a field attenuation test. The arrow shows the frequency of the applied external field which had an amplitude of 2 gauss. Data represents 6 hours of integration.

4. Acknowledgments

This work is supported by NASA contract NAS8-36125 from the George C. Marshall Space Flight Center.

We wish to acknowledge the support of the whole Gravity Probe-B team at Stanford and Lockheed. The following individuals have been particularly instrumental in the success of FIST: From Stanford: F. Alkemade, P. Bayer, M. Bye, D. Charleston, J. Gill, C. Gray, R. Hacker, L. V. Ho, P. Lindener, H. Malekian, M. McGirvin, A. Ortega, T. Quinn, J. Stamets, T. Van Hooydonk, and C. Warren; From

Lockheed: E. Cavity, D. Donegan, C. Everson, J. Goodman, D. Harshman, W. Hewitt, E. Iufer, K. Kasunic, A. Kelly, M. Mintz, J. Nauss, M. Regelbrugge, L. Sands, P. Spencer, D. Welsh, E. Will, and S. Yuan. In addition, D. Davidson of Optical Instrument Design has played a crucial role in the design and fabrication of many quartz components.

5. References

1. L. I. Schiff, *Proc. Nat. Acad. Sci.* **46**, 871 (1960); also *Phys. Rev. Lett.* **4**, 215 (1960).
2. For an introduction to GP-B and an historical overview, see C. W. F. Everitt in *Near Zero: New Frontiers of Physics*, ed. J. D. Fairbank, *et al.* (W. H. Freeman, New York, 1988) p. 587.
3. For a more detailed overview of the development key GP-B technologies, see D. Bardas, *et al.*, *Proc. SPIE* **619**, 29 (1986).
4. A more detailed discussion of the GP-B gyro design and fabrication can be found in J. P. Turneaure, *et al.*, *Adv. Space Res.* **9**, 29 (1989) and references therein.
5. For a more detailed discussion of the gyro readout see J. M. Lockhart, *Proc. SPIE* **619**, 148 (1986), and J. T. Anderson in *Near Zero: New Frontiers of Physics*, ed. J. D. Fairbank, *et al.* (W. H. Freeman, New York, 1988) p. 659.
6. F. London, *Superfluids, Vol. 1: Macroscopic Theory of Superconductivity* (Dover, New York, 1961).
7. Details of the telescope can be found in C. W. F. Everitt, D. E. Davidson, R. A. Van Patten, *Proc. SPIE* **619**, 148 (1986).
8. P. M. Selzer, W. M. Fairbank, C. W. F. Everitt, *Adv. Cry. Eng.* **16**, 277 (1971)
9. The first demonstration of the drag-free zero-g concept was with the U.S. Navy's TRIAD Transit Navigation Satellite reported on by the staffs of the Space Dept. of the Johns Hopkins University Applied Physics Laboratory and the Guidance and Control Laboratory of Stanford University in *J. Spacecraft and Rockets* **11**, 637 (1974).
10. J. P. Turneaure, E. A. Cornell, P. D. Levine, J. A. Lipa in *Near Zero: New Frontiers of Physics*, ed. J. D. Fairbank, *et al.* (W. H. Freeman, New York, 1988) p. 671.
11. B. Cabrera in *Near Zero: New Frontiers of Physics*, ed. J. D. Fairbank, *et al.* (W. H. Freeman, New York, 1988) p. 312; also discussed in the first paper of ref. 5.
12. Details of the dewar and probe design are included in the paper by R. T. Parmley and G. M. Reynolds in the proceedings of this meeting.
13. Some details of the FIST design may be found in D. Bardas, *et al.*, *Proceedings of the Fifth Marcel Grossmann Meeting on General Relativity*, ed. D. G. Blair, M. J. Buckingham (World Scientific, Singapore, 1989) p. 1633.
14. SQUID sensors were manufactured by Biomagnetic Technologies, Inc., and the readout electronics were made by Quantum Design, Inc.